The Arabidopsis KS-type dehydrin recovers lactate dehydrogenase activity inhibited by copper with the contribution of His residues

doi: 10.1016/j.plantsci.2016.02.006

Title page

Original research paper

Title

The *Arabidopsis* KS-type dehydrin recovers lactate dehydrogenase activity inhibited by copper with the contribution of His residues.

Authors

Masakazu Hara[a*], Shuhei Monna[a], Takae Murata[a], Taiyo Nakano[a], Shono Amano[a], Markus Nachbar[b], Hermann Wätzig[b]

[a]Research Institute of Green Science and Technology,
Shizuoka University,
836 Ohya, Shizuoka 422-8529, Japan

[b]Institut für Pharmazeutische Chemie,
Technische Universität Braunschweig,
Beethovenstraße 55, 38106 Braunschweig, Germany

***Name and address for editorial correspondence**

Masakazu Hara
Research Institute of Green Science and Technology,
Shizuoka University,
836 Ohya, Shizuoka 422-8529, Japan
Telephone number: +81-54-238-5134
Fax number: +81-54-238-5134
E-mail address: hara.masakazu@shizuoka.ac.jp

Abstract

Dehydrin, which is one of the late embryogenesis abundant (LEA) proteins, is involved in the ability of plants to tolerate the lack of water. Although many reports have indicated that dehydrins bind heavy metals, the physiological role of this metal binding has not been well understood. Here, we report that the *Arabidopsis* KS-type dehydrin (AtHIRD11) recovered the lactate dehydrogenase (LDH) activity denatured by Cu^{2+}. The LDH activity was partially inhibited by 0.93 μM Cu^{2+} but totally inactivated by 9.3 μM Cu^{2+}. AtHIRD11 recovered the activity of LDH treated with 9.3 μM Cu^{2+} in a dose-dependent manner. The recovery activity of AtHIRD11 was significantly higher than those of serum albumin and lysozyme. The conversion of His residues to Ala in AtHIRD11 resulted in the loss of the Cu^{2+} binding of the protein as well as the disappearance of the conformational change induced by Cu^{2+} that is observed by circular dichroism spectroscopy. The mutant protein showed lower recovery activity than the original AtHIRD11. These results indicate that AtHIRD11 can reactivate LDH inhibited by Cu^{2+} via the His residues. This function may prevent physiological damage to plants due to heavy-metal stress.

Keywords

Copper

Dehydrin

Heavy metal

His

1. Introduction

Plants which are exposed to abiotic stresses produce diverse proteins to prevent damage caused by the stresses. Dehydrin, a group 2 late embryogenesis abundant protein, is such a protein. Various plant species produce dehydrins during embryogenesis and stress responses, including drought, cold, and high salinity. Many reviews have summarized the amino acid sequence characteristics, expression patterns, cellular and subcellular localizations, and physiological functions of dehydrins (see reviews such as [1-8]). A dehydrin is defined by the presence of conserved K-segment(s). The typical sequence of a K-segment is EKKGIMDKIKEKLPG, which is anticipated to form an amphipathic helix [1-8]. Dehydrins frequently have other domains, i.e. a Y-segment (a typical sequence; DEYGNP) and S-segment (LHRSGSSSSSSEDD or related sequences). A convenient shorthand is available to classify dehydrins using the K, Y, and S-segments, such as SKn, KnS, Kn, YnSKn, YnKn, etc. It is suggested that SKn, KnS, and Kn dehydrins are remarkably up-regulated by cold stress but that

YnSKn and YnKn dehydrins are mainly upregulated by desiccation stress [8]. Since dehydrins are rich in hydrophilic residues over their whole sequences, the proteins show a highly flexible structure, indicating that they are intrinsically disordered proteins [1-8]. This structural feature has been demonstrated by circular dichroism (CD), Fourier-transform infrared spectroscopy (FTIR), and nuclear magnetic resonance (NMR) [9, 10]. Dehydrins are widely distributed in various subcellular compartments, such as the cytoplasm, nucleus, plasma membrane, tonoplast, plastid, mitochondrion, endoplasmic reticulum, etc. [1-8]. Although dehydrins have been frequently detected in the vasculature, more ubiquitous expression has been found in stressed cells [11-14].

In the early stage of the study of dehydrins, functional studies were limited due to the highly disordered conformation and the low sequence similarity to proteins whose functions were known. Recent studies have provided evidence that dehydrins contribute to the establishment of stress tolerance in plants. Transgenic analyses revealed that dehydrins enhanced stress tolerances, protection from damage caused by low temperature [15-20], osmotic stress [21-24], and high salinity [25] tolerances. The results of the transgenic studies have been supported by molecular functional analyses. Dehydrins exhibited cryoprotection [1-8] and dehydration protection [26] of enzymes. Dehydrins showed an affinity to phospholipids [27-30] and water [31]. These functions may be directly related to the enhancement of cold and drought tolerances in plants. In addition, calcium binding [32, 33] and nucleic acid binding [34, 35] have been demonstrated, although it is unclear how the calcium and nucleic acid bindings participate in the stress tolerance.

In this way dehydrins have been studied as water stress-related proteins. On the other hand, dehydrins have also been investigated as heavy-metal binders. Svensson et al. found that various recombinant *Arabidopsis* dehydrins showed affinity to heavy metals in immobilized metal ion affinity chromatography (IMAC) [36]. Krüger et al. reported that a metal transporter purified from the phloem of young *Ricinus communis* plants was demonstrated to be a KS-type dehydrin [37]. The His-rich sequence (HKGEHHSGDHH) was determined to be the Cu^{2+}-binding domain of the *Citrus* K_2S-type dehydrin CuCOR15 [38]. These results imply that dehydrins may inhibit heavy-metal toxicity in plants. In general, the direct toxicity caused by heavy metals can be categorized as either (1) the production of reactive oxygen species (ROS) or (2) the inhibition of the functions of biomolecules [39]. We previously demonstrated that dehydrin prevented the former toxicity due to heavy metals, i.e. the production of ROS. The *Arabidopsis* KS-type dehydrin AtHIRD11 efficiently inhibited the generation of ROS from copper [40]. The activity of AtHIRD11 was more potent than those of radical-silencing peptides such as glutathione and serum albumin. However, no research has been conducted on preventing the heavy-metal-promoting dysfunction of biomolecules by dehydrin. In this paper, we report that

AtHIRD11 efficiently recovered the lactate dehydrogenase (LDH) activity denatured by Cu^{2+}, and the His residues contributed to the recovery activity. We discuss the putative roles of dehydrins in heavy-metal detoxification in plants.

2. Materials and methods

2.1. Chemicals

Soybean lipoxygenase (LOX), yeast glutathione reductase (GR), bovine catalase (CAT), bovine serum albumin (BSA), and lysozyme were purchased from Sigma (Tokyo, Japan). Horseradish peroxidase (POD) and $CuCl_2$ were obtained from Wako (Tokyo, Japan). Rabbit LDH was purchased from Oriental Yeast (Tokyo, Japan).

2.2. Treatment of enzymes with Cu^{2+}

Five enzymes (i.e., LOX, GR, POD, CAT, and LDH) were prepared as follows. LOX (2 μg/mL, 100 U/mL), CAT (40 μg/mL, 160 U/mL), and POD (40 μg/mL, 8 U/mL) were dissolved in 10 mM Tris-HCl buffer pH 7.5. GR (1 μg/mL, 0.2 U/mL) and LDH (1.7 μg/mL, 0.68 U/mL) were prepared in 50 mM sodium phosphate buffer pH 7.5 and 100 mM sodium phosphate buffer pH 6.8, respectively. The definition of U in each enzyme is described below. The enzyme solutions (1.6 μL) were combined with $CuCl_2$ (0.8 μL, at the concentrations of 4.63, 46.3, 463, and 4630 μM). As a control, 0.8 μL of water was added instead of the $CuCl_2$ solutions. After mixing for 30 sec, water (1.6 μL) was added to the samples. At this stage, the final concentrations of $CuCl_2$ were 0.926, 9.26, 92.6, and 926 μM, respectively. The Cu^{2+}-treated enzyme samples (4 μL of total volume) were subjected to the corresponding enzyme assays described below.

2.3. Enzyme assays

All enzyme assays were performed according to the methods described in the manufacturer's instructions with modifications. The LOX sample (4 μL) was combined with the substrate solution (196 μL, 100 mM Tris-HCl buffer pH 7.5 containing 12 mM linoleate and 5% Tween20). The reaction was monitored at 234 nm with a microplate reader (Varioskan Flash, Thermo Fisher Scientific, Tokyo, Japan) at 25 ^{o}C. One U was defined as 0.12 nmol linoleate oxidized per min. The GR sample (4 μL) was mixed with the substrate solution (196 μL, 50 mM sodium phosphate buffer pH 7.5 containing 1 mM ethylene diamine tetraacetic acid, 1 mM

oxidized glutathione, and 0.1 mM NADPH), and then absorption at 340 nm was recorded with the Varioskan Flash microplate reader. One unit was defined as a reduction of 1 μmol oxidized glutathione per min. The CAT sample (4 μL) was added to the substrate solution (196 μL, 10 mM Tris-HCl buffer pH 7.5 containing 18 mM hydrogen peroxide). The decrease of the hydrogen peroxide concentration was monitored at 240 nm. The same microplate reader was used. One U represents a reduction of 1 μmol hydrogen peroxide per min. For the POD assay, the reaction was started by mixing the POD sample (4 μL) and the substrate solution (196 μL, 10 mM Tris-HCl buffer pH 7.5 containing 6 mM guaiacol and 2.6 mM hydrogen peroxide). An absorbance at 470 nm was recorded using the microplate reader. One unit was defined as the amount of enzyme which oxidizes 1 μmol guaiacol per min. The LDH sample (4 μL) was combined with the substrate solution (100 mM sodium phosphate buffer pH 6.8 containing 0.81 mM sodium pyruvate and 0.22 mM NADH). The absorbance was recorded at 340 nm. The same microplate reader was used for monitoring. One unit was defined as the amount of enzyme which converts 1 μmol pyruvate to lactate per min.

2.4. Effect of dehydrins on LDH activity

To test the effect of proteins on the LDH activity, 1.6 μL of LDH (4.25 μg/mL, 1.7 U/mL) was combined with 0.8 μL of $CuCl_2$ (0 μM for the control and 46.3 μM for the treatment). After mixing for 30 sec, 1.6 μL of proteins was added to the samples. The enzymatic activity of the LDH mixture (4 μL of total volume) was determined as described above. The proteins were AtHIRD11, BSA, lysozyme, AtHIRD11_FLAG, and AtHIRD11_H/A_FLAG. The final concentrations were 0.926, 9.26, 92.6, and 926 μM.

2.5. Preparation of recombinant proteins

AtHIRD11 was produced according to the method described previously [41]. The procedure is briefly described here. The cDNA encoding AtHIRD11 was inserted into the pET-30 *Escherichia coli* expression vector (Novagen, WI, USA). The recombinant AtHIRD11 with the His- and S- tags was expressed in the *E. coli* strain BL21. Crude proteins extracted from the bacterial cells were heated at 90^{o}C for 20 min. After centrifugation, the supernatant containing the recombinant AtHIRD11 was treated with Factor Xa (Novagen) to remove the tags. AtHIRD11 was purified by HiTrap Chelating HP column charged with Ni^{2+} (GE Healthcare, Tokyo, Japan) followed by DEAE-Toyopearl 650 M (Tosoh, Tokyo, Japan). The purified AtHIRD11 was desalted and freeze-dried. The protein was identified using a matrix-assisted laser desorption/ionization time-of-flight mass spectrometry (MALDI-TOF-MS) system

composed of a 4700 Proteomics Analyzer (Applied Biosystems, Tokyo, Japan).

Chemical DNA synthesis was applied to produce the cDNA sequences encoding AtHIRD11_FLAG and AtHIRD11_H/A_FLAG (Takara Bio, Shiga, Japan). The cDNAs were inserted into the pET-30 vectors. AtHIRD11_FLAG and AtHIRD11_H/A_FLAG were prepared by the same method as the production of AtHIRD11 described above except that the HiTrap Chelating HP column chromatography was omitted in the case of AtHIRD11_H/A_FLAG. The purified proteins were identified using the same MALDI-TOF-MS described above and immunoblotted with anti-FLAG antibody (Sigma).

2.6. Immobilized metal ion affinity chromatography (IMAC)

IMAC was performed using a 1-mL HiTrap Chelating HP (GE, Tokyo, Japan) column which was connected to the EGP system (Bio-Rad, Tokyo, Japan) according to the method described previously [38]. The column was charged by applying 3 ml of 100 mM $CuCl_2$ followed by 5 ml of deionized water to wash out the excess metal. After equilibrating the column with 25 mM Tris–HCl buffer pH 7.5 containing 0.5 M NaCl (1/2EQ buffer), recombinant proteins, i.e. AtHIRD11, AtHIRD11_FLAG, or AtHIRD11_H/A_FLAG (50 μM, 100 μL), were applied to the column. The unbound protein was washed out with 5 mL of 1/2EQ buffer, and then eluted by a linear gradient of imidazole (0-1 M in 26 mL of 1/2EQ buffer). Fractions (1 mL each) were analyzed by SDS-PAGE stained with Coomassie blue (Bio-Safe, Bio-Rad). Band intensity was determined using NIH-image software (http://rsb.info.nih.gov/nih-image/), and relative band intensity was calculated.

2.7. Circular dichroism (CD)

Conformational changes of AtHIRD11, AtHIRD11_FLAG, and AtHIRD11_H/A_FLAG by Cu^{2+} were analyzed by means of CD. The proteins (4.6 μM) and $CuCl_2$ (0, 2.3, and 23 μM) were combined in 10 mM Tris-HCl pH 7.5. After incubating for 5 min at room temperature, the samples were analyzed with a spectropolarimeter (J-820, Jasco, Tokyo, Japan). The scan was performed from 195 to 250 nm three times. The scan speed, resolution, and cell width were 100 nm min^{-1}, 1 nm, and 2 mm, respectively.

2.8. Statistical analysis

Data for *P* values were analyzed by Student's *t* test at a significance level of 0.05.

3. Results

3.1. Inhibition of enzymatic activity by Cu^{2+}

First, we identified an enzyme sensitive to heavy metal in order to investigate whether dehydrin can recover a metal-inactivated enzyme. Here we used copper because excess copper inhibits plant growth by interfering with physiological processes such as enzyme activity [42]. Since LDH is known as a copper-sensitive enzyme [43], we measured the LDH activity under different concentrations of Cu^{2+} as well as other oxidoreductases such as LOX, GR, POD, and CAT. The concentrations of Cu^{2+} were 0 (no-treatment control), 0.93, 9.3, 93, and 930 μM (Fig. 1). Although POD, CAT, and LDH activities were inhibited by Cu^{2+}, LOX and GR activities were not. LDH was the most sensitive to Cu^{2+} among the oxidoreductases tested in this study. The LDH activities were lowered to 27% and 2.2% of the control activity by the addition of 0.93 μM and 9.3 μM Cu^{2+}, respectively. Based on these results, we decided to use the combination of LDH and Cu^{2+} as the enzyme system inhibited by heavy metal. The Cu^{2+} concentration of 9.3 μM was used to inactivate LDH in the following experiments.

3.2. Effect of dehydrin on LDH inactivated by Cu^{2+}

In this work, we used AtHIRD11, which is a KS-type dehydrin of *Arabidopsis* (At1g54410). AtHIRD11, which is the smallest in size (98 amino acids) among the 10 *Arabidopsis* dehydrins, was abundantly expressed in the plant [41]. The orthologues are common in higher plants such as *Ricinus communis*, *Glycine max*, *Solanum sogarandinum*, *Oryza sativa*, *Medicago sativa*, *Vitis vinifera*, etc. [41, 44].

First, we tested whether AtHIRD11 influences the activity of LDH in the absence of Cu^{2+}. AtHIRD11 (0, 0.093, 0.93, 9.3, and 93 μM) was combined with LDH (30 nM), indicating that AtHIRD11 at concentrations up to 0.93 μM did not influence the LDH activities (Fig. 2). AtHIRD11, however, enhanced the LDH activity at the higher concentrations (9.3 and 93 μM). Next, the effect of AtHIRD11 on the Cu^{2+}-inactivated LDH was investigated. When AtHIRD11 was added to LDH treated with 9.3 μM Cu^{2+}, AtHIRD11 recovered the LDH activity with dose dependency (Fig. 3). AtHIRD11 at 9.3 μM recovered the Cu^{2+}-inactivated LDH to the initial activity of LDH. The activity of Cu^{2+}-treated LDH exceeded the initial activity by 93 μM AtHIRD11. In addition, Zn^{2+} also inhibited the LDH activity in a dose-dependent manner, but the inhibition activity of Zn^{2+} was lower than that of Cu^{2+} (Supplemental Fig. 1A). AtHIRD11 at 93 μM efficiently recovered the LDH activity inhibited by 930 μM Zn^{2+} (Supplemental Fig. 1B).

To investigate whether other proteins rather than AtHIRD11 also show recovery activities for

Cu^{2+}-inactivated LDH, we tested BSA and lysozyme as standard proteins (Fig. 4). Although BSA and lysozyme showed recovery activities, their activities were lower than that of AtHIRD11. The relative activities of LDH after the addition of BSA and lysozyme were approximately 45% and 18% of the relative activity in AtHIRD11, respectively, when compared at the concentration of 9.3 μM.

3.3. Contribution of His residues to the LDH recovery

It was demonstrated that His residues are involved in the heavy-metal binding of dehydrins [38]. This implies that the His residues are also related to the recovery activity of AtHIRD11 for the Cu^{2+}-inactivated LDH. We changed the His residues of AtHIRD11 to Ala to investigate the contribution of His to the recovery activity of LDH by AtHIRD11. The sequences of the original AtHIRD11 and the mutant proteins are shown in Fig. 5. The original AtHIRD11 has 13 His residues (Fig. 5, AtHIRD11). At the first trial, we prepared a mutant protein in which all His residues were changed to Ala. However, our anti-AtHIRD11 antibody could not recognize the mutant protein, probably because the recognition sequence of the antibody, i.e., EHKKEEEHKKHVDEHKSGE [41], was altered by the substitution. This led to difficulties in purifying the mutant protein. Thus we produced a mutant protein in which a FLAG sequence was added at the C-terminus (Fig. 5, AtHIRD11_H/A_FLAG). We also produced AtHIRD11 with FLAG at the C-terminus (Fig. 5, AtHIRD11_FLAG) to offset the effect of the FLAG addition. These mutant proteins were detected by immunoblotting with the anti-FLAG antibody (Supplemental Fig. 2).

We compared the strength of Cu^{2+} binding among AtHIRD11, AtHIRD11_FLAG, and AtHIRD11_H/A_FLAG using IMAC chelating Cu^{2+} (Fig. 6). AtHIRD11 and AtHIRD11_FLAG were retained in the Cu^{2+} column and eluted with imidazole gradient. On the other hand, most of the AtHIRD11_H/A_FLAG passed through the Cu^{2+} column. This indicates that AtHIRD11 and AtHIRD11_FLAG bound Cu^{2+}, but AtHIRD11_H/A_FLAG almost lost the capability of binding. Equilibrium binding experiments revealed that the dissociation constants (K_ds) of AtHIRD11 and AtHIRD11_FLAG were 3.3 and 1.1 μM, respectively. However, the maximum bindings (B_{max}s) of AtHIRD11 and AtHIRD11_FLAG were equal in value (7.8 mol mol^{-1}) (Fig. 6, Supplemental Fig. 3). It is likely that the attachment of the FLAG sequence altered the binding affinity of AtHIRD11 to Cu^{2+}, whereas the binding capacities were not influenced.

It was reported that AtHIRD11 showed a conformational change induced by Cu^{2+} [40]. Previous CD analysis indicated that AtHIRD11 showed a disordered state with a large negative peak around 200 nm, but the disordered conformation was attenuated by the addition of Cu^{2+}. In this work, we collected the CD data of AtHIRD11, AtHIRD11_FLAG, and

AtHIRD11_H/A_FLAG under the presence or absence of Cu^{2+} (Fig. 7). The values of the negative peaks around 200 nm in AtHIRD11 and AtHIRD11_FLAG increased concomitant with the increase in the Cu^{2+} concentrations (Figs. 7A and B). The CD spectrum of AtHIRD11_H/A_FLAG, however, was not influenced by the addition of Cu^{2+} (Fig. 7C). This shows that the His residues are related to the Cu^{2+}-promoting conformational changes of AtHIRD11.

We determined the abilities of AtHIRD11, AtHIRD11_FLAG, and AtHIRD11_H/A_FLAG to recover the Cu^{2+}-inactivated LDH. AtHIRD11_FLAG recovered the LDH activity to a degree similar to AtHIRD11 (Fig. 8). AtHIRD11_H/A_FLAG, however, showed significantly lower recovery activity than AtHIRD11. This indicates that the His residues in the AtHIRD11 sequence participate in the activity by which the Cu^{2+}-inactivated LDH is recovered.

The calculated model suggested that the coordination of 7 Cu^{2+} ions to AtHIRD11 provided the most stable conformation (Supplemental Fig. 4). In this modeling, the 6 Cu^{2+} ions out of the 7 Cu^{2+} ions could be bound by the corresponding 6 His residues, i.e. His31, His40, His53, His82, His87, and His88. However, another Cu^{2+} ion was bound via Glu63 and Glu79. The maximum Cu^{2+} bindings of AtHIRD11 was 7.8 mol mol^{-1} in the equilibrium binding analyses as above, suggesting that 1 Cu^{2+} ion can be bound between 2 AtHIRD11 molecules or 8 Cu^{2+} ions can be bound to AtHIRD11 in spite of providing more instability than the coordination of 7 Cu^{2+} ions.

4. Discussion

Since dehydrins are related to drought and cold stresses, the functions of dehydrins have been studied in the context of how they protect cells against these stresses. In addition, many reports have documented the heavy-metal binding of dehydrins [36-38, 45, 46], suggesting that dehydrins may prevent metal toxicity in plants [47]. This idea has been supported by the following findings: metal tolerance was promoted by tobacco expressing the *Brassica* dehydrins [48] and the copper sensitivity of the yeast *sod1* (Cu/Zn superoxide dismutase) mutant was complemented by *Musa* dehydrin [45]. These results show that at least some dehydrins can prevent heavy-metal stress in plants.

Regarding heavy-metal stress, two major mechanisms, i.e., the generation of ROS and the dysfunction of biomolecules (e.g., enzymes), are generally accepted [39]. In a previous work we demonstrated that AtHIRD11 inhibited the ROS generation from copper and that His residues were necessary for the ROS inhibition [40]. The present work indicates the recovery of LDH inactivated by Cu^{2+}. To assess whether the His residues of AtHIRD11 contribute to reactivating the Cu^{2+}-inactivated LDH, we produced an artificial protein (AtHIRD11_H/A_FLAG) in which all His residues were changed to Ala (Fig. 5, AtHIRD11_H/A_FLAG). We obtained the

following results; AtHIRD11_H/A_FLAG showed remarkably lower recovery of the Cu^{2+}-inactivated LDH than AtHIRD11 and AtHIRD11_FLAG, AtHIRD11 and AtHIRD11_FLAG bound Cu^{2+} but AtHIRD11_H/A_FLAG did not, and AtHIRD11 and AtHIRD11_FLAG showed conformational changes induced by Cu^{2+} but AtHIRD11_H/A_FLAG showed little change. These results suggest that AtHIRD11 recovered the Cu^{2+}-inactivated LDH by binding Cu^{2+} concomitant with conformational change via the His residues. We propose that AtHIRD11 inhibits the ROS generation and enzyme inactivation which are promoted by heavy metals; therefore, AtHIRD11 may ameliorate the physiological disorder caused by heavy metals (Fig. 9).

It is known that the KnS-type dehydrins possess a high proportion of His in their sequences: e.g., 13.3% (*Arabidopsis* AtHIRD11), 13.9% (*Citrus* CuCOR15), and 19.0% (*Ricinus* ITP) [49]. These values are abnormally high, because the occurrence of His residues in general proteins is approximately 2% [50]. Other types of dehydrins also contain a higher proportion of His residues than in general proteins, such as the Kn-type (*Arabidopsis* Lti30, 13.5%), the SKn-type (*Arabidopsis* COR47, 4.9%), the YnSKn (*Arabidopsis* Rab18, 4.3%), etc. [49]. Considering the high contents of His in dehydrins, it is likely that preventing heavy-metal stress is a common function of dehydrins, whereas the efficiency of stress prevention may vary among dehydrins. Recent studies have demonstrated that His residues are related to the lipid interaction and the nuclear localization of dehydrins [29, 51]. Taken together, these findings suggest that His makes important contributions to the functions of dehydrins.

LDH converts lactate to pyruvate by using NAD^+ as a cofactor. In the active site of LDH the His residue donates an electron via its imidazole ring to the hydroxyl group of lactate to dehydrate it [52]. Although the mechanism by which Cu^{2+} inhibits LDH activity remains undefined, Cu^{2+} can interact with the His residue to inhibit the electron donation. AtHIRD11 may reactivate the Cu^{2+}-inactivated LDH by removing Cu^{2+} from the active site using the His residues. Because Cu^{2+} promotes the self-association of AtHIRD11 [40], Cu^{2+} from LDH may be spatially sequestered to the self-association particles. From another point of view, the removal of Cu^{2+} from the Cu^{2+}-inactivated enzymes by AtHIRD11 may promote folding of the inactivated enzymes by molecular chaperones, because heavy metals prevent the chaperone-assisted refolding of denatured proteins [53].

The concentration of tetrameric LDH used in this study was 30 nM. Cu^{2+} partially inhibited the LDH activity at the concentration of 0.93 μM, but wholly inactivated LDH at 9.3 μM (Fig. 1). AtHIRD11 at 9.3 μM could fully recover the LDH activity inactivated by 9.3 μM Cu^{2+} (Fig. 3). Since AtHIRD11 binds 7-8 Cu^{2+} ions [41], the excess amount of AtHIRD11 may be necessary to remove Cu^{2+} from the Cu^{2+}-inactivated LDH.

Figure 4 indicated that BSA and lysozyme also recovered the Cu^{2+}-inactivated LDH. It is

known that serum albumin is the major transporter of Cu^{2+} in blood. BSA can bind Cu^{2+} [54] by the ATCUN motif ($+NH_3$-X-X-His) [55]. Lysozyme is noted to bind Cu^{2+} as well [56]. However, the recovery activities of BSA and lysozyme for the Cu^{2+}-inactivated LDH were significantly lower than that of AtHIRD11 (Fig. 4). This may be because AtHIRD11 possesses many His residues accessible for Cu^{2+} ions as revealed by the computational model (Supplemental Fig. 4). In other words, AtHIRD11 likely exposes more His residues to the outer environment than BSA and lysozyme do.

It is unclear whether the reduction of heavy-metal toxicity by dehydrins contributes to enhancing water-stress tolerance in plants. Under water stress, heavy metals are released from metal proteins and concentrated in the dehydrated cytoplasm [57]. The concentrated heavy metals may cause ROS production and enzyme inactivation, both of which promote physiological damage in plants. This suggests that water stress may be related to heavy-metal stress. It is likely that in plants dehydrins may enhance water-stress tolerance by ameliorating heavy-metal toxicity.

Recently, it has been argued that dehydrins may protect enzymes under freezing conditions by acting as molecular shields [58]. The highly flexible structure of dehydrins seems to be important for the effective cryoprotection of LDH, because polyethylene glycol (PEG), which is an artificial flexible polymer, showed the same level of cryoprotection as dehydrins [59]. It has been reported that the K-segments are related to the cryoprotection provided by dehydrins [8], suggesting that the K-segments prevent enzyme inactivation due to freezing and that the His residues protect enzymes from inactivation caused by heavy metals. This shows that dehydrins can be multi-functional enzyme protectors (i.e., cryoprotection and recovery from heavy-metal inactivation) that stabilize the physiological activities of plant cells under stress conditions.

Acknowledgements

This study was supported by a Grant-in-Aid (No. 23380192) for Scientific Research from the Ministry of Education, Science, Sports and Culture of Japan.

References

[1] T.J. Close, Dehydrins: Emergence of a biochemical role of a family of plant dehydration proteins, Physiol. Plant. 97 (1996) 795-803.

[2] T. Rorat, Plant dehydrins: tissue location, structure and function, Cell Mol. Biol. Lett. 11 (2006) 536-556.

[3] M. Battaglia, Y. Olvera-Carrillo, A. Garciarrubio, F. Campos, A.A. Covarrubias, The enigmatic LEA proteins and other hydrophilins, Plant Physiol. 148 (2008) 6-24.

[4] M. Hundertmark, D.K. Hincha, LEA (Late Embryogenesis Abundant) proteins and their encoding genes in *Arabidopsis thaliana*. BMC Genomics 9 (2008) 118.

[5] S.K. Eriksson, P. Harryson, Dehydrins: Molecular Biology, Structure and Function, in: U. Lüttge, E. Beck, D. Bartels, (Eds.), Plant Desiccation Tolerance, Springer Berlin Heidelberg, 2011, pp. 289-305.

[6] M. Hanin, F. Brini, C. Ebel, Y. Toda, S. Takeda, K. Masmoudi, Plant dehydrins and stress tolerance: versatile proteins for complex mechanisms, Plant Signal. Behav. 6 (2011) 1503-1509.

[7] X. Sun, E.H. Rikkerink, W.T. Jones, V.N. Uversky, Multifarious roles of intrinsic disorder in proteins illustrate its broad impact on plant biology, Plant Cell 25 (2013) 38-55.

[8] S.P. Graether, K.F. Boddington, Disorder and function: a review of the dehydrin protein family, Front. Plant Sci. 5 (2014) 576.

[9] L.N. Rahman, G.S. Smith, V.V. Bamm, J.A. Voyer-Grant, B.A. Moffatt, J.R. Dutcher, G. Harauz, Phosphorylation of *Thellungiella salsuginea* dehydrins TsDHN-1 and TsDHN-2 facilitates cation-induced conformational changes and actin assembly, Biochemistry 50 (2011) 9587-9604.

[10] B. Szalainé Ágoston, D. Kovács, P. Tompa, A. Perczel, Full backbone assignment and dynamics of the intrinsically disordered dehydrin ERD14, Biomol. NMR Assign. 5 (2011) 189-193.

[11] J.A. Godoy, R. Lunar, S. Torres-Schumann, J. Moreno, R.M. Rodrigo, J.A. Pintor-Toro, Expression, tissue distribution and subcellular localization of dehydrin TAS14 in salt-stressed tomato plants, Plant Mol. Biol. 26 (1994) 1921-1934.

[12] J. Danyluk, A. Perron, M. Houde, A. Limin, B. Fowler, N. Benhamou, F. Sarhan, Accumulation of an acidic dehydrin in the vicinity of the plasma membrane during cold acclimation of wheat, Plant Cell 10 (1998) 623-638.

[13] L.A. Bravo, T.J. Close, L.J. Corcuera, C.L. Guy, Characterization of an 80-kDa dehydrin-like protein in barley responsive to cold acclimation, Physiol. Plant. 106 (1999) 177-183.

[14] M. Nylander, J. Svensson, E.T. Palva, B.V. Welin, Stress-induced accumulation and tissue-specific localization of dehydrins in *Arabidopsis thaliana*, Plant Mol. Biol. 45 (2001) 263-279.

[15] M. Hara, S. Terashima, T. Fukaya, T. Kuboi, Enhancement of cold tolerance and inhibition of lipid peroxidation by citrus dehydrin in transgenic tobacco, Planta 217 (2001) 290-298.

[16] T. Puhakainen, M.W. Hess, P. Mäkelä, J. Svensson, P. Heino, E.T. Palva, Overexpression of multiple dehydrin genes enhances tolerance to freezing stress in Arabidopsis, Plant Mol. Biol. 54 (2004) 743-753.

[17] M. Houde, S. Dallaire, D. N'Dong, F. Sarhan, Overexpression of the acidic dehydrin WCOR410 improves freezing tolerance in transgenic strawberry leaves, Plant Biotechnol. J. 2 (2004) 381-387.

[18] Z. Yin, T. Rorat, B.M. Szabala, A. Ziólkowska, S. Malepszy, Expression of a *Solanum sogarandinum* SK3-type dehydrin enhances cold tolerance in transgenic cucumber seedlings, Plant Sci. 170 (2006) 1164-1172.

[19] X. Xing, Y. Liu, X. Kong, Y. Liu, D. Li, Overexpression of a maize dehydrin gene, ZmDHN2b, in tobacco enhances tolerance to low temperature, Plant Growth Regul. 65 (2011) 109-118.

[20] A.E. Ochoa-Alfaro, M. Rodríguez-Kessler, M.B. Pérez-Morales, P. Delgado-Sánchez, C.L. Cuevas-Velazquez, G. Gómez-Anduro, J.F. Jiménez-Bremont, Functional characterization of an acidic SK3 dehydrin isolated from an *Opuntia streptacantha* cDNA library, Planta 235 (2012) 565-578.

[21] Z. Cheng, J. Targolli, X. Huang, R. Wu, Wheat LEA genes, PMA80 and PMA1959 enhance dehydration tolerance of transgenic rice (*Oryza sativa* L.), Mol. Breed. 10 (2002) 71-82.

[22] M. Figueras, J. Pujal, A. Saleh, R. Save, M. Pagès, A. Goday, Maize Rab17 overexpression in *Arabidopsis* plants promotes osmotic stress tolerance, Annal. Appl. Biol. 144 (2004) 251-257.

[23] F. Brini, M. Hanin, V. Lumbreras, I. Amara, H. Khoudi, A. Hassairi, M. Pagès, K. Masmoudi, Overexpression of wheat dehydrin DHN-5 enhances tolerance to salt and osmotic stress in *Arabidopsis thaliana*, Plant Cell Rep. 26 (2007) 2017-2026.

[24] Y. Wang, H. Wang, R. Li, Y. Ma, J. Wei, Expression of a SK2-type dehydrin gene from *Populus euphratica* in a *Populus tremula* × *Populus alba* hybrid increased drought tolerance, Afr. J. Biotechnol. 10 (2011) 9225-9232.

[25] U.K. Shekhawat, L. Srinivas, T.R. Ganapathi, MusaDHN-1, a novel multiple stress-inducible SK(3)-type dehydrin gene, contributes affirmatively to drought- and salt-stress tolerance in banana, Planta 234 (2011) 915-932.

[26] M. Drira, W. Saibi, F. Brini, A. Gargouri, K. Masmoudi, M. Hanin, The K-segments of the wheat dehydrin DHN-5 are essential for the protection of lactate dehydrogenase and β-glucosidase activities in vitro, Mol. Biotechnol. 54 (2013) 643-650.

[27] M.C. Koag, S. Wilkens, R.D. Fenton, J. Resnik, E. Vo, T.J. Close, The K-segment of maize DHN1 mediates binding to anionic phospholipid vesicles and concomitant structural changes, Plant Physiol. 150 (2009) 1503-1514.

[28] D. Kovacs, E. Kalmar, Z. Torok, P. Tompa, Chaperone activity of ERD10 and ERD14, two disordered stress-related plant proteins, Plant Physiol. 147 (2008) 381-390.

[29] S.K. Eriksson, M. Kutzer, J. Procek, G. Gröbner, P. Harryson, Tunable membrane binding of the intrinsically disordered dehydrin Lti30, a cold-induced plant stress protein, Plant Cell 23 (2011) 2391-2404.

[30] L.N. Rahman, F. McKay, M. Giuliani, A. Quirk, B.A. Moffatt, G. Harauz, J.R. Dutcher, Interactions of *Thellungiella salsuginea* dehydrins TsDHN-1 and TsDHN-2 with membranes at cold and ambient temperatures-surface morphology and single-molecule force measurements show phase separation, and reveal tertiary and quaternary associations, Biochim. Biophys. Acta. 1828 (2013) 967-980.

[31] P. Tompa, P. Bánki, M. Bokor, P. Kamasa, D. Kovács, G. Lasanda, K. Tompa, Protein-water and protein-buffer interactions in the aqueous solution of an intrinsically unstructured plant dehydrin: NMR intensity and DSC aspects, Biophys. J. 91 (2006) 2243-2249.

[32] B.J. Heyen, M.K. Alsheikh, E.A. Smith, C.F. Torvik, D.F. Seals, S.K. Randall, The calcium-binding activity of a vacuole-associated, dehydrin-like protein is regulated by phosphorylation, Plant Physiol. 130 (2002) 675-687.

[33] M.K. Alsheikh, J.T. Svensson, S.K. Randall, Phosphorylation regulated ion-binding is a property shared by the acidic subclass dehydrins, Plant Cell Environ. 28 (2005) 1114-1122.

[34] M. Hara, Y. Shinoda, Y. Tanaka, T. Kuboi, DNA binding of citrus dehydrin promoted by zinc ion, Plant Cell Environ. 32 (2009) 532-541.

[35] C.H. Lin, P.H. Peng, C.Y. Ko, A.H. Markhart, T.Y. Lin, Characterization of a novel Y2K-type dehydrin VrDhn1 from *Vigna radiata*, Plant Cell Physiol. 53 (2012) 930-942.

[36] J. Svensson, E.T. Palva, B. Welin, Purification of recombinant *Arabidopsis thaliana* dehydrins by metal ion affinity chromatography, Protein Exp. Purif. 20 (2000) 169-178.

[37] C. Krüger, O. Berkowitz, U.W. Stephan, R. Hell, A metal-binding member of the late embryogenesis abundant protein family transports iron in the phloem of *Ricinus communis* L, J. Biol. Chem. 277 (2002) 25062-25069.

[38] M. Hara, M. Fujinaga, T. Kuboi, Metal binding by citrus dehydrin with histidine-rich domains, J. Exp. Bot. 56 (2005) 2695-2703.

[39] A. Schützendübel, A. Polle, Plant responses to abiotic stresses: heavy metal-induced oxidative stress and protection by mycorrhization, J. Exp. Bot. 53 (2002) 1351-1365.

[40] M. Hara, M. Kondo, T. Kato, A KS-type dehydrin and its related domains reduce Cu-promoted radical generation and the histidine residues contribute to the radical-reducing activities, J. Exp. Bot. 64 (2013) 1615-1624.

[41] M. Hara, Y. Shinoda, M. Kubo, D. Kashima, I. Takahashi, T. Kato, T. Horiike, T. Kuboi, Biochemical characterization of the *Arabidopsis* KS-type dehydrin protein, whose gene

expression is constitutively abundant rather than stress dependent, Acta Physiol. Plant. 33 (2011) 2103-2116.

[42] J.C. Fernandes, F.S. Henriques, Biochemical, physiological and structure effects of excess copper in plants, Botanical Rev. 57 (1991) 246-273.

[43] N. Verma, M. Singh, Biosensors for heavy metals, Biometals 18 (2005) 121-129.

[44] T. Rorat, W.J. Grygorowicz, W. Irzykowski, P. Rey, Expression of KS-type dehydrins is primarily regulated by factors related to organ type and leaf developmental stage during vegetative growth, Planta 218 (2004) 878-885.

[45] P. Mu, D. Feng, J. Su, Y. Zhang, J. Dai, H. Jin, B. Liu, Y. He, K. Qi, H. Wang, J. Wang, Cu^{2+} triggers reversible aggregation of a disordered His-rich dehydrin MpDhn12 from *Musa paradisiaca*, J. Biochem. 150 (2011) 491-499.

[46] L.N. Rahman, G.S. Smith, V.V. Bamm, J.A. Voyer-Grant, B.A. Moffatt, J.R. Dutcher, G. Harauz, Phosphorylation of *Thellungiella salsuginea* dehydrins TsDHN-1 and TsDHN-2 facilitates cation-induced conformational changes and actin assembly, Biochemistry 50 (2011) 9587-9604.

[47] M. Hara, The multifunctionality of dehydrins: An overview, Plant Signal. Behav. 5 (2010) 503-508.

[48] J. Xu, Y.X. Zhang, W. Wei, L. Han, Z.Q. Guan, Z. Wang, T.Y. Chai, BjDHNs confer heavy-metal tolerance in plants, Mol. Biotechnol. 38 (2008) 91-98.

[49] X. Sun, H.H. Lin, Role of plant dehydrins in antioxidation mechanisms, Biologia 65 (2010) 755-759.

[50] E.K. Ueda, P.W. Gout, L. Morganti, Current and prospective applications of metal ion-protein binding, J. Chromatogr. A. 988 (2003) 1-23.

[51] I.E. Hernández-Sánchez, I. Maruri-López, A. Ferrando, J. Carbonell, S.P. Graether, J.F. iménez-Bremont, Nuclear localization of the dehydrin OpsDHN1 is determined by histidine-rich motif. Front. Plant Sci. 6 (2015) 702.

[52] M.J. Adams, M. Buehner, K. Chandrasekhar, G.C. Ford, M.L. Hackert, A. Liljas, M.G. Rossmann, I.E. Smiley, W.S. Allison, J. Everse, N.O. Kaplan, S.S. Taylor, Structure-function relationships in lactate dehydrogenase, Proc. Natl. Acad. Sci. U.S.A. 70 (1973) 1968-1972.

[53] S.K. Sharma, P. Goloubinoff, P. Christen, Heavy metal ions are potent inhibitors of protein folding, Biochem. Biophys. Res. Commun. 372 (2008) 341-345.

[54] S. Redweik, C. Cianciulli, M. Hara, Y. Xu, H. Wätzig, Precise, fast and flexible determination of protein interactions by affinity capillary electrophoresis. Part 2: cations, Electrophoresis 34 (2013) 1812-1819.

[55] C. Harford, B. Sarkar, Amino terminal Cu(II)- and Ni(II)-binding (ATCUN) motif of proteins and peptides: metal binding, DNA cleavage, and other properties, Acc. Chem. Res. 30 (1997) 123-130.

[56] F.Y. Lin, W.Y. Chen, L.C. Sang, Microcalorimetric studies of the interactions of lysozyme with immobilized metal ions: Effects of ion, pH value, and salt concentration, J. Colloid Interface Sci. 214 (1999) 373-379.

[57] I. Iturbe-Ormaetxe, P.R. Escuredo, C. Arrese-Igor, M. Becana, Oxidative damage in pea plants exposed to water deficit or paraquat, Plant Physiol. 116 (1998) 173-181.

[58] S. Hughes, S.P. Graether, Cryoprotective mechanism of a small intrinsically disordered dehydrin protein, Protein Sci. 20 (2011) 42-50.

[59] S.L. Hughes, V. Schart, J. Malcolmson, K.A. Hogarth, D.M. Martynowicz, E. Tralman-Baker, S.N. Patel, S.P. Graether, The importance of size and disorder in the cryoprotective effects of dehydrins, Plant Physiol. 163 (2013) 1376-1386.

Figure legends

Fig. 1. Effects of Cu^{2+} on enzymatic activities. Lipoxygenase (LOX), glutathione reductase (GR), peroxidase (POD), catalase (CAT), and lactate dehydrogenase (LDH) were used. The Cu^{2+} concentrations were 0 (control), 0.93, 9.3, 93, and 930 μM. Values and bars represent means ± SD. Four individual experiments were performed. Relative enzyme activities are

shown as %. Activities of non-treated enzymes are standardized (100%). Asterisks show significant differences ($p < 0.05$) as determined by Student's *t*-test in a comparison between no treatment (0 μM) and Cu^{2+} treatments.

Fig. 2. Effect of AtHIRD11 on lactate dehydrogenase (LDH) activity. AtHIRD11 at different concentrations was added to LDH. Values and bars represent means ± SD (four individual experiments). Relative enzyme activities are shown as %. Activities of non-treated enzymes are standardized (100%). Asterisks show significant differences ($p < 0.05$) as determined by Student's *t*-test in a comparison between no treatment (0 μM) and AtHIRD11 treatments.

Fig. 3. Recovery of the Cu^{2+}-inhibited lactate dehydrogenase (LDH) activity by AtHIRD11. After LDH was inactivated by 9.3 μM Cu^{2+}, different concentrations of AtHIRD11 were added, and the LDH activities were measured. Values and bars represent means ± SD (four individual experiments). Relative enzyme activities are shown as %. Activities of non-treated enzymes are standardized (100%). Asterisks show significant differences ($p < 0.05$) as determined by Student's *t*-test in a comparison between no treatment and AtHIRD11 treatments. Mole numbers of AtHIRD11 per 1 mole of Cu^{2+} are shown in parentheses.

Fig. 4. Recovery of the Cu^{2+}-inhibited lactate dehydrogenase (LDH) activity by proteins. After LDH was inactivated by 9.3 μM Cu^{2+}, different concentrations of AtHIRD11 (black columns), bovine serum albumin (gray columns), and lysozyme (white columns) were added, and the LDH activities were measured. Values and bars represent means ± SD (four individual experiments). Relative enzyme activities are shown as %. Activities of non-treated enzymes are standardized (100%). Asterisks show significant differences ($p < 0.05$) as determined by Student's *t*-test in a comparison between AtHIRD11 and other proteins in each concentration. Mole numbers of proteins per 1 mole of Cu^{2+} are shown in parentheses.

Fig. 5. Amino acid sequences of AtHIRD11, AtHIRD11_FLAG, and AtHIRD11_H/A_FLAG. K-, PK-, and S-segments in the original AtHIRD11 are represented as bidirectional arrows. Broken underlines show FLAG. His residues in AtHIRD11 and AtHIRD11_FLAG are underlined. The Ala residues in AtHIRD11_H/A_FLAG to which His residues in AtHIRD11_FLAG were changed are underlined.

Fig. 6. Cu^{2+} bindings of AtHIRD11, AtHIRD11_FLAG, and AtHIRD11_H/A_FLAG. Immobilized metal ion affinity chromatography was used. The protein amount in each fraction is shown as a relative band intensity in SDS-PAGE. The sum of band intensities was set to

100%. Values and bars represent means ± SD (three individual experiments). Broken lines indicate the imidazole gradient (0-1 M). K_ds and B_{max}s determined by equilibrium binding assay are represented in the graphs of AtHIRD11 and AtHIRD11_FLAG. Details of the equilibrium binding assay are shown in Supplemental Fig. 3.

Fig. 7. Effect of Cu^{2+} on the conformations of AtHIRD11, AtHIRD11_FLAG, and AtHIRD11_H/A_FLAG. Circular dichroism (CD) was measured when different concentrations of $CuCl_2$ were added to the proteins. Gray solid lines (4.6 μM proteins with 0 μM Cu^{2+}), black broken lines (4.6 μM proteins with 2.3 μM Cu^{2+}), and black solid lines (4.6 μM proteins with 23 μM Cu^{2+}) are shown. A typical record out of three measurements in each protein is exhibited.

Fig. 8. Recovery of the Cu^{2+}-inhibited lactate dehydrogenase (LDH) activity by AtHIRD11, AtHIRD11_FLAG, and AtHIRD11_H/A_FLAG. After LDH was inactivated by 9.3 μM Cu^{2+}, different concentrations of AtHIRD11 (black columns), AtHIRD11_FLAG (gray columns), and AtHIRD11_H/A_FLAG (white columns) were added, and then the LDH activities were measured. Values and bars represent means ± SD (four individual experiments). Relative enzyme activities are shown as %. Activities of non-treated enzymes are standardized (100%). Asterisks show significant differences ($p < 0.05$) as determined by Student's *t*-test in a comparison between AtHIRD11 and other proteins in each concentration. Mole numbers of AtHIRD11, AtHIRD11_FLAG, and AtHIRD11_H/A_FLAG per 1 mole of Cu^{2+} are shown in parentheses.

Fig. 9. Hypothetical scheme of the dehydrin function for preventing heavy-metal toxicity in plants. Heavy metals cause physiological disorders through ROS generation, enzyme inactivation, and other effects. Dehydrin may inhibit the ROS generation [40] and enzyme inactivation (this study) via His, which is a metal-binding residue.

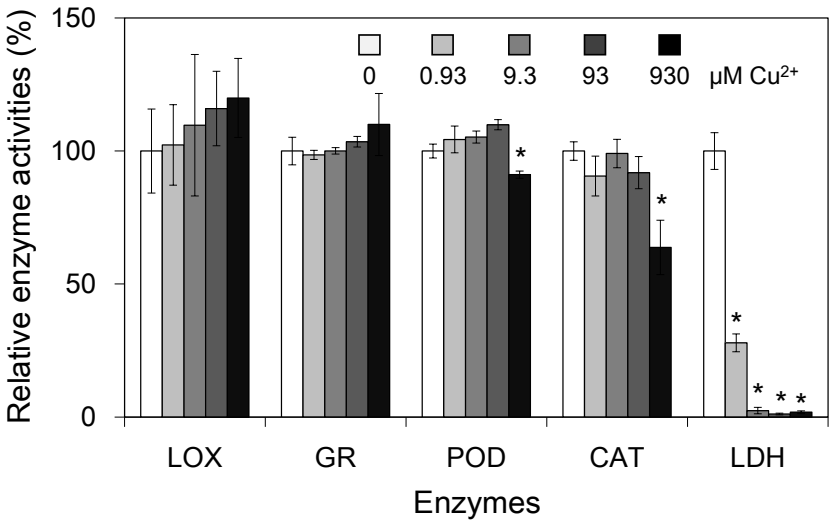

Fig. 1 Hara et al.

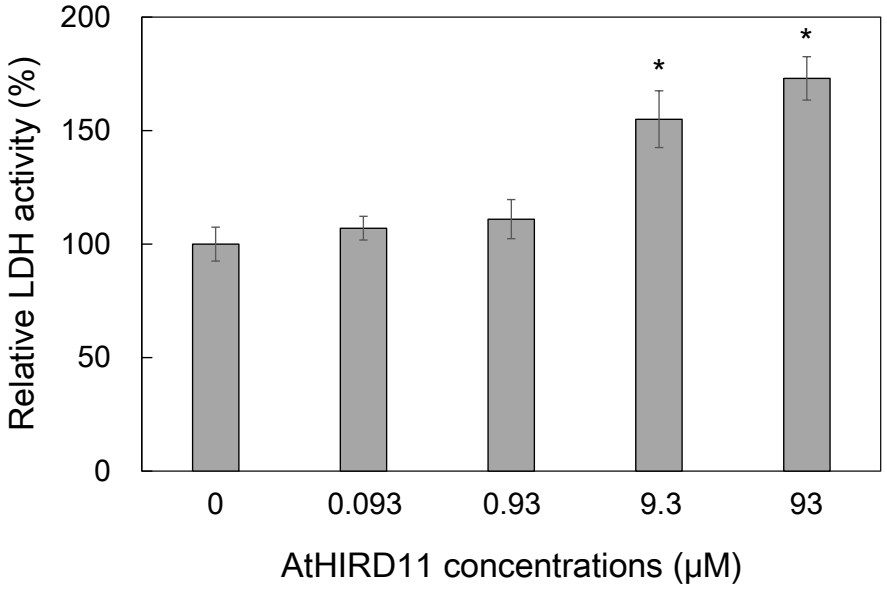

Fig. 2 Hara et al.

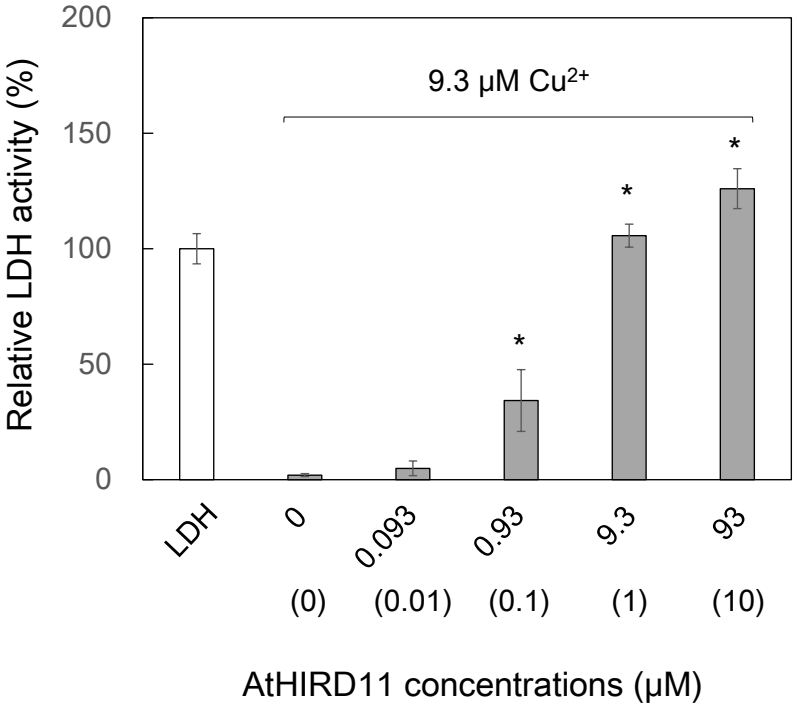

Fig. 3 Hara et al.

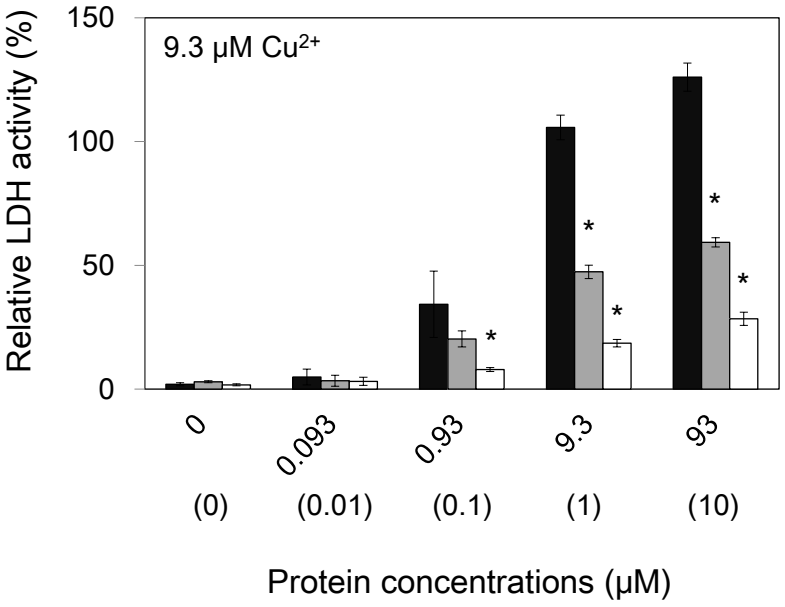

Fig. 4 Hara et al.

AtHIRD11

MAGLNKIGDALHIGGGNKEGEHKKEEEHKKHVDEHKSGEHKEGIVDKIKDKIHGG

K-seg

EGKSHDGEGKSHDGEKKKKKDKKEKKHHDDGHHSSSSDSDSD

PK-seg S-seg

AtHIRD11_FLAG

MAGLNKIGDALHIGGGNKEGEHKKEEEHKKHVDEHKSGEHKEGIVDKIKDKIHGG
EGKSHDGEGKSHDGEKKKKKDKKEKKHHDDGHHSSSSDSDSDYKDDDDK

FLAG

AtHIRD11_H/A_FLAG

MAGLNKIGDALAIGGGNKEGEAKKEEEAKKAVDEAKSGEAKEGIVDKIKDKIAGG
EGKSADGEGKSADGEKKKKKDKKEKKAADDGAASSSSDSDSDYKDDDDK

FLAG

Fig. 5 Hara et al.

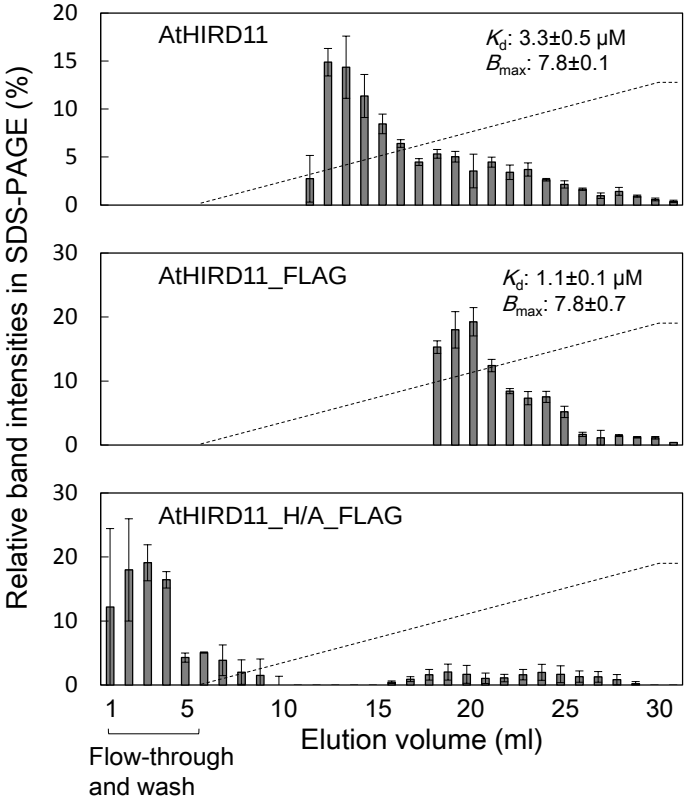

Fig. 6 Hara et al.

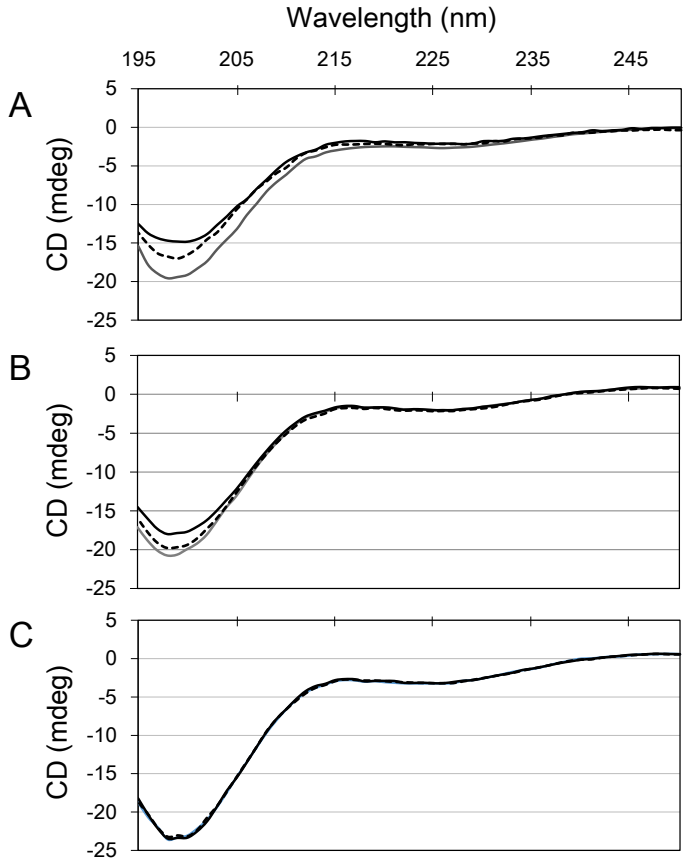

Fig. 7 Hara et al.

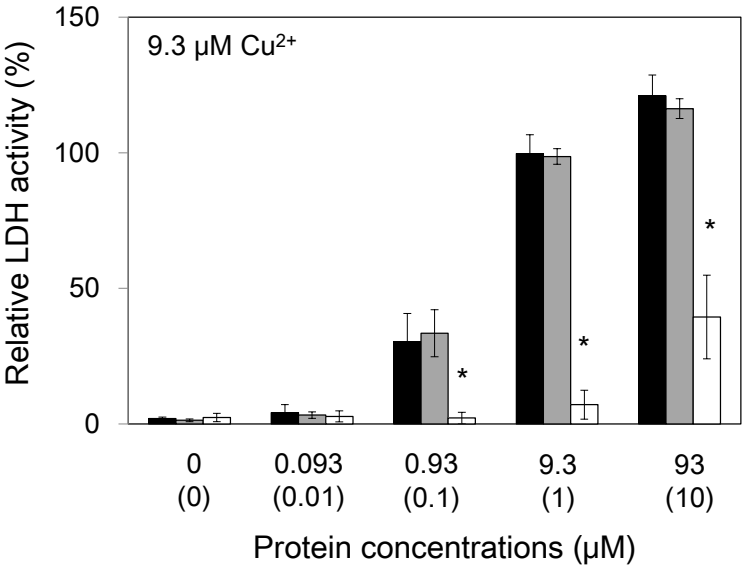

Fig. 8 Hara et al.

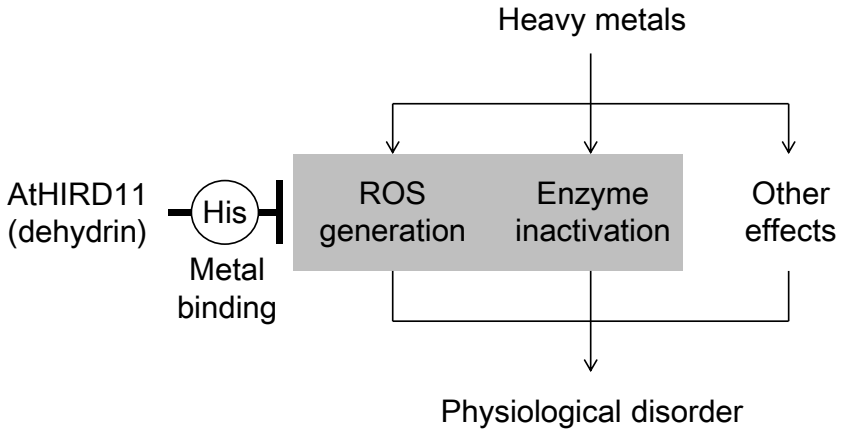

Fig. 9 Hara et al.

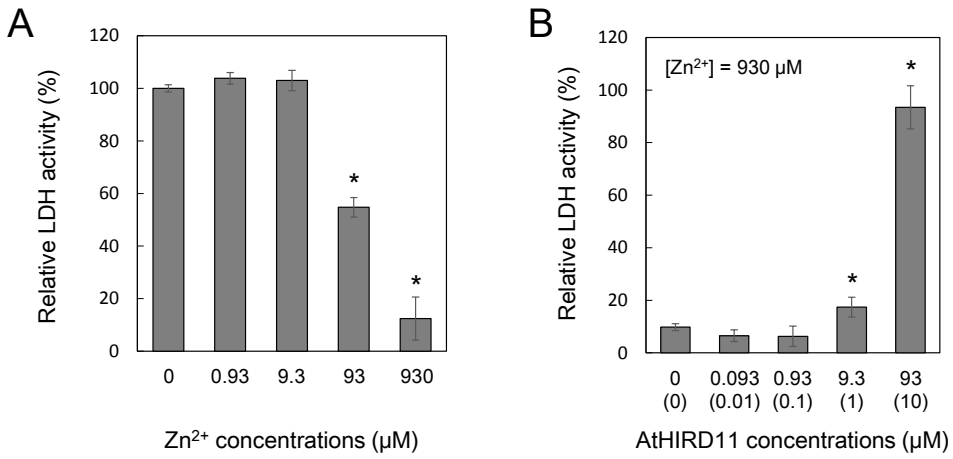

Supplemental Fig. 1. Hara et al.

(A) Effect of Zn^{2+} on lactate dehydrogenase (LDH) activity. Values and bars represent means ± SD (4 individual experiments). Relative enzyme activities are shown as %. Activities of non-treated enzymes are standardized (100%). Asterisks show significant differences ($p < 0.05$) as determined by Student's t-test in a comparison between no treatment (0 μM) and Zn^{2+} treatments. The LDH solution (4.25 μg/mL, 1.7 U/mL) was prepared in 100 mM sodium phosphate buffer at a pH of 6.8. This enzyme solution (1.6 μL) was combined with $ZnCl_2$ (0.8 μL, at various concentrations). As a control, 0.8 μL of water was added instead of the $ZnCl_2$ solutions. After mixing for 30 sec, water (1.6 μL) was added to the samples. At this stage, the final concentrations of $ZnCl_2$ were 0.926, 9.26, 92.6, and 926 μM, respectively. The Zn^{2+}-treated enzyme samples (4 μL of total volume) were subjected to the LDH assay described in the text. (B) Recovery of the Zn^{2+}-inhibited lactate dehydrogenase (LDH) activity by AtHIRD11. After LDH was inactivated by 930 μM Zn^{2+}, different concentrations of AtHIRD11 were added, and the LDH activities were measured. Values and bars represent means ± SD (four individual experiments). Relative enzyme activities are shown as %. Activities of non-treated enzymes are standardized (100%). Asterisks show significant differences ($p < 0.05$) as determined by Student's t-test in a comparison between no treatment and AtHIRD11 treatments. Mole numbers of AtHIRD11 per 1 mole of Zn^{2+} are shown in parentheses. For enzyme assays 1.6 μL of LDH (4.25 μg/mL, 1.7 U/mL) was combined with 0.8 μL of $ZnCl_2$ (0 μM for the control and 463 μM for the treatment). After mixing for 30 sec, AtHIRD11 (1.6 μL at various concentrations) was added to the samples. The LDH activity of the mixture (4 μL of total volume) was determined as described above. The final concentrations of AtHIRD11 were 0.0926, 0.926, 9.26, and 92.6 μM, respectively.

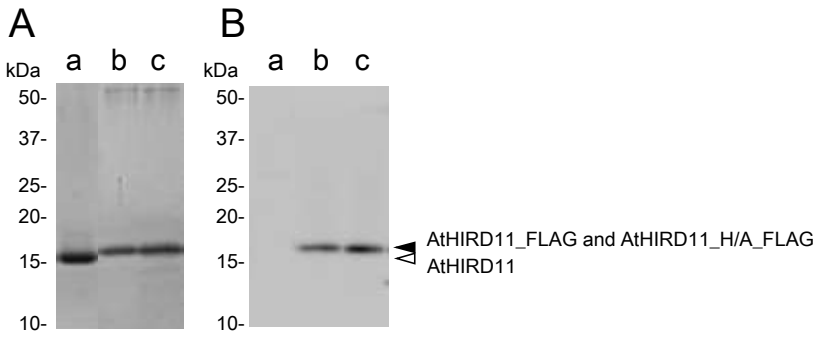

Supplemental Fig. 2. Hara et al.

AtHIRD11-related recombinant proteins used in this study. AtHIRD11 (a), AtHIRD11_FLAG (b), and AtHIRD11_H/A_FLAG (c). The purified proteins were analyzed by sodium dodecyl sulfate-polyacrylamide gel electrophoresis stained with Coomassie blue (Bio-Safe, Bio-Rad, Tokyo, Japan) (A) and by immunoblotting with anti-FLAG antibody (Sigma, Tokyo, Japan) using the Immun-Star chemiluminescent system (Bio-Rad) (B). (A) AtHIRD11 (1 μg), AtHIRD11_FLAG (0.7 μg), and AtHIRD11_H/A_FLAG (0.7 μg) were loaded. (B) AtHIRD11 (10 ng), AtHIRD11_FLAG (7 ng), and AtHIRD11_H/A_FLAG (7 ng) were loaded.

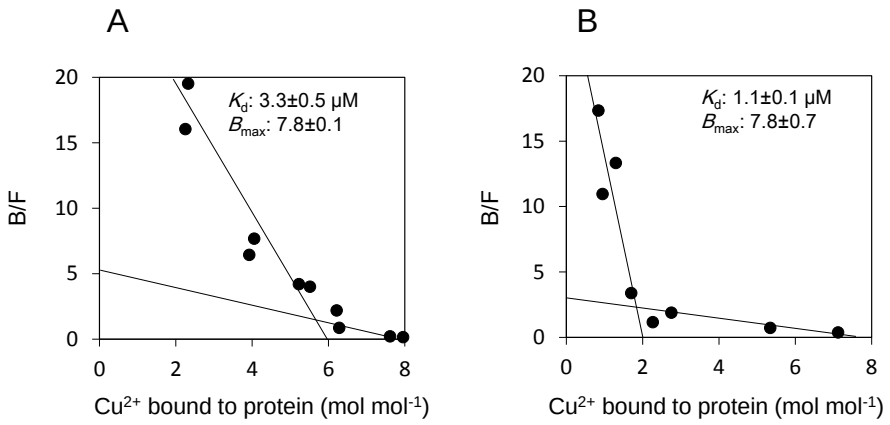

Supplemental Fig. 3. Hara et al.

Cu^{2+} bindings of AtHIRD11 (A) and AtHIRD11_FLAG (B) were analyzed by Scatchard plots. Mixtures (final volume; 0.5 mL) containing 16.7 μM AtHIRD11 or AtHIRD11_FLAG, 10 mM Tris–HCl pH 7.5, 100 mM NaCl, and various concentrations (25–650 μM) of $CuCl_2$ were incubated at 4°C for 10 min. The mixture was subjected to ultrafiltration (Ultrafree-MC, 5000 NMWL, Millipore, 4,000xg for 30 min at 4°C). The concentrations of free metals which passed through the filter were determined using a 2-(5-bromo-2-pyridylazo)-5-(N-propyl-N-sulfopropylamino)phenol (5-Br-PAPS) (Dojindo Chemical, Tokyo, Japan) assay. The free (F) and bound (B) metal concentrations were determined, and then the B/F values were calculated. The typical plots are shown. K_ds and B_{max}s are shown as means ± SD (3 individual experiments). Microsoft Excel 2007 was used to fit linear equations.

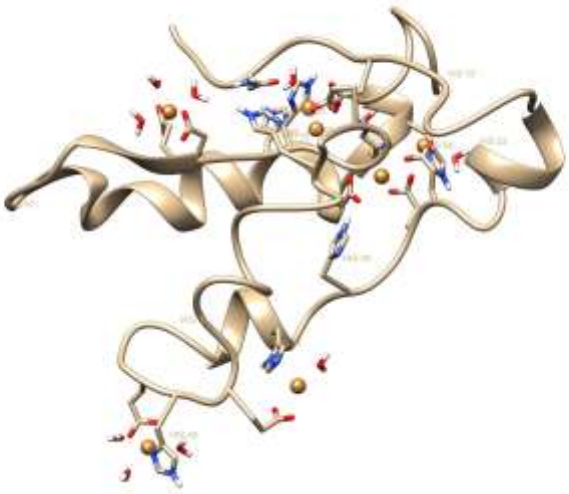

Supplemental Fig. 4. Hara et al.

Homology model for the AtHIRD11-Cu^{2+}-complex. For illustration of the AtHIRD11 ternary structure, a homology model was set up using the molecular modelling software MOE (Chemical Computing Group, Montreal, Canada). Since the alignment of the AtHIRD11 amino acid sequence and the sequence of the His-phosphotransferase domain of the *Escherichia coli* protein barA (pdb identifier: 3IQT) gave a similarity of roughly 30%, the His-phosphotransferase domain was used as a template for creating the model. Afterwards, Cu^{2+} ions were inserted at possible binding sites, the bond lengths as well as the bond angles were optimized, and a molecular dynamics simulation was performed using the GROMACS (D. Van Der Spoel, E. Lindahl, B. Hess, G. Groenhof, A.E. Mark, H.J. Berendsen, GROMACS: fast, flexible, and free, J. Comput. Chem. 26 (2005) 1701-1718) force field GROMOS53a6ff. For visualization of the results and determination of the deviation from the ideal geometry, the UCSF Chimera 1.8.1 software (E.F. Pettersen, T.D. Goddard, C.C. Huang, G.S. Couch, D.M. Greenblatt, E.C. Meng, T.E. Ferrin, UCSF Chimera - a visualization system for exploratory research and analysis, J. Comput. Chem. 25 (2004) 1605–1612.) was used.